EFFICIENCY IMPROVEMENTS OF SEVENTH-ORDER WEIGHTED COMPACT NONLINEAR SCHEME

Taku Nonomura[†] , Weipeng Li[‡], Yoshinori Goto[‡♯] and Kozo Fujii[†]

Abstract

Efficiency improvements of high-order weighted compact nonlinear scheme (WCNS) are discussed using a one-dimensional shock entropy-wave interaction problem. Computational efficiencies of schemes are evaluated with computational time and error compared with a reference solution. Seventh-order WCNS with eighth-order explicit differencing is used as a base scheme. A couple of techniques improving resolution and reducing computational cost are discussed. Series of tests show that WCNS with both localization of nonlinear-weight computation and relative limiter has the best performance on the test problem. Finally, the most efficient WCNS is applied to three-dimensional CFD/CAA problems, and improvements in computation cost and resolution of modified WCNS are verified.

Key Words: Weighted Compact Nonlinear Scheme, Relative limiter, Mapped technique, Convex Combined Compact Scheme

1 INTRODUCTION

High-order shock-capturing schemes are required for efficient and stable computation of complex flow fields that contains discontinuities and turbulence. Especially, finite difference schemes are preferred because they require only dimension-by-dimension procedure which is computationally cheaper than multi-dimensional reconstruction used in finite volume and finite element schemes.[1]

Weighted compact nonlinear scheme (WCNS) was developed by Deng and Zhang,[2] which is high-resolution finite difference scheme for the flow fields containing the discontinuities. WCNS has several advantages compared with finite difference weighted essentially nonoscillatory scheme(WENO)[3] as follows: i) variable interpolation and approximate Riemann solver can be used in WCNS despite it is a finite difference scheme;[2] ii) WCNS can preserve freestream while WENO cannot;[5] iii) WCNS has higher resolution than WENO.[2,4] Though original WCNS is fifth-order scheme, higher-order WCNSs, up to ninth, were introduced by Nonomura et al.[6] and Zhang et al.[4], independently.

However, the resolution of high-order WCNS for short waves is lower than that of linear compact scheme, and WCNS is computationally very expensive compared with linear schemes. In other words, high-order WCNS efficiency still does not seem to be enough for accurate large-eddy simulations or direct numerical simulations of turbulent flow fields. Therefore, it is necessary to improve efficiency of WCNS for practical simulations. Thus far, several computational techniques improving efficiency of WENO or WCNS has been proposed. In the present paper, seventh-order WCNS is modified with these techniques and their efficiencies are discussed using Shu and Osher's shock entropy-wave interaction problem[7]. Finally, the most efficient WCNS is applied to three-dimensional CFD/CAA problems, and efficiency improvements are verified compared with original WCNS.

Received on.

† Institute of Space and Astronautical Science, Japan Aerospace Exploration Agency.
‡ Department of Aeronautics and Astronautics, University of Tokyo.
♯ Currently TOYOTA Motor Company.

2 Seventh-Order WCNS with Modifications

Nonomura et al.[6] and Zhang et al.[4] developed high-order WCNSs, independently. Nonomura et al. increased order of WCNS more straightforwardly from the original fifth-order WCNS. In this study, WCNS developed by Nonomura et al. is used because the techniques which improves resolution of original WCNS are simply applicable to WCNS developed by Nonomura et al., but not to WCNS developed by

Zhang et al. Order of accuracy is set to seventh because seventh-order WCNS is the most efficient among fifth-, seventh- and ninth-order WCNSs in our a priori computational tests.

2.1 Original WCNS

Now, we consider the one-dimensional Euler equation as follows.

$$\frac{\partial Q}{\partial t}+\frac{\partial E}{\partial x}=0 \tag{1}$$

$$Q=(\rho,\rho u,\rho e)^T \tag{2}$$

$$E=(\rho u,\rho u^2+p,(\rho e+p)u)^T \tag{3}$$

WCNS has three procedures for computing approximate derivatives; 1) interpolating flow-variables from computational nodes to mid-points, 2) evaluating numerical fluxes at mid-points, and 3) differencing numerical fluxes at mid-points with a high-order (compact/explicit) linear scheme. These procedures are briefly explained.

1)interpolate the flow-variables from the computational node to the mid-point

For simplicity, interpolation of $Q^L_{j+1/2}$ is only explained. Interpolation of $Q^R_{j+1/2}$ can be symmetrically computed. Seventh-order WCNS adopts a seventh-order weighted interpolation. Seventh-order weighted interpolation uses a 7-points stencil $\{Q_{j-3},\cdots,Q_{j+3}\}$. First, conservative variable Q is transformed into characteristic variables q in the stencil. Then, m-th component of $q^{L,k,m}_{j+1/2}$ $(k=1,\ldots,4)$ is computed by k-th 4-points sub-stencil as follows.

$$q^{L,1,m}_{j+1/2}=-\frac{5}{16}q^m_{j-3}+\frac{21}{16}q^m_{j-2}-\frac{35}{16}q^m_{j-1}+\frac{35}{16}q^m_j \tag{4}$$

$$q^{L,2,m}_{j+1/2}=\frac{1}{16}q^m_{j-2}-\frac{5}{16}q^m_{j-1}+\frac{15}{16}q^m_j+\frac{5}{16}q^m_{j+1} \tag{5}$$

$$q^{L,3,m}_{j+1/2}=-\frac{1}{16}q^m_{j-1}+\frac{9}{16}q^m_j+\frac{9}{16}q^m_{j+1}+\frac{1}{16}q^m_{j+2} \tag{6}$$

$$q^{L,4,m}_{j+1/2}=\frac{5}{16}q^m_j+\frac{15}{16}q^m_{j+1}-\frac{5}{16}q^m_{j+2}+\frac{1}{16}q^m_{j+3} \tag{7}$$

Next, $q_{j+1/2,m}$ is computed as a weighted average of $q^{L,k,m}_{j+1/2}$.

$$\begin{aligned}q^{L,m}_{j+1/2}=&w_1q^{L,1,m}_{j+1/2}+w_{2,m}q^{L,2,m}_{j+1/2}\\&+w_3q^{L,3,m}_{j+1/2}+w_{4,m}q^{L,4,m}_{j+1/2}\end{aligned} \tag{8}$$

where w_k is a nonlinear weight computed as follows.

$$w_{k,m}=\frac{\alpha_{k,m}}{\sum_l \alpha_{l,m}} \tag{9}$$

$$\alpha_{k,m}=\frac{C_k}{(IS_{k,m}+\varepsilon)^2} \tag{10}$$

Here, $(C_1,C_2,C_3,C_4)=(1/64,21/64,35/64,7/64)$ are ideal weights, and $IS_{k,m}$ is a smooth indicator computed as follows.

$$IS_{k,m}=\sum_{n=1}^{4}\left(\sum_{l=1}^{4}c_{n,k,l}q^m_{j+k+l-5}\right) \tag{11}$$

where $c_{n,k,l}$ is a coefficient for a smooth indicator. In seventh-order WCNS by Nonomura et al., eqs. (4-7,11) are simply computed using approximate derivatives to reduce computational cost. See Reference [6] for more details. Finally, $q^L_{j+1/2}$ is transformed into $Q^L_{j+1/2}$.

2)evaluate the numerical fluxes on the mid point

Numerical flux is evaluated with the following equation.

$$E^{WCNS}_{j+1/2}=F_{FLUX}(Q^L_{j+1/2},Q^R_{j+1/2}) \tag{12}$$

where F_{FLUX} is an arbitrary flux evaluation method, e.g. Roe's flux difference splitting method,[8] Leer's flux vector splitting method,[9] or Liou's advection upstream splitting method.[10]

3) difference numerical fluxes on the mid point with the high-order linear scheme

Finally, first derivative of flux is computed with a high-order linear difference scheme. The type of this difference scheme (explicit/compact) does not have strong effects on resolution of WCNS.[11,12] In this study, an eighth-order explicit difference scheme is used as follows.

$$\begin{aligned}E'_j=&\frac{1}{\Delta x}\frac{1225}{1024}(E^{WCNS}_{j+1/2}-E^{WCNS}_{j-1/2})\\&-\frac{1}{\Delta x}\frac{245}{3072}(E^{WCNS}_{j+3/2}-E^{WCNS}_{j-3/2})\\&+\frac{1}{\Delta x}\frac{49}{5120}(E^{WCNS}_{j+5/2}-E^{WCNS}_{j-5/2})\\&-\frac{1}{\Delta x}\frac{5}{7168}(E^{WCNS}_{j+7/2}-E^{WCNS}_{j-7/2})\end{aligned} \tag{13}$$

2.2 Mapping Technique

Nonlinear weights in WENO are not always appropriate values in smooth region. For improving resolution at smooth region, mapping technique[14] is used for WENO. The mapping technique introduces new weighted averaging instead of original weighted averaging.

$$q^{L,m}_{j+1/2}=w^M_{1,m}q^{L,1,m}_{j+1/2}+w^M_{2,m}q^{L,2,m}_{j+1/2}$$

$$+ w_{3,m}^{M} q_{j+1/2}^{L,3,m} + w_{4,m}^{M} q_{j+1/2}^{L,4,m} \tag{14}$$

where $w_{k,m}^{M}$ is a mapped weight computed as follows.

$$w_{k,m}^{M} = \frac{w_{k,m}\left(C_k + (C_k)^2 - 3C_k w_{k,m} + (w_{k,m})^2\right)}{(C_k)^2 - (1-2C_k)\, w_{k,m}} \tag{15}$$

With the above formulation, resolution of WENO scheme becomes higher. See Reference [13] for more details. This technique is applied to WCNS and its efficiency is examined in this paper. This scheme is called WCNSM.

2.3 Relative Limiter

Similar to mapping technique, relative limiter[15] increases resolution of WENO. Relative limiter is used for the smooth indicator of WENO. A new smooth indicator $IS_{k,m}^{RL}$ is used instead of $IS_{k,m}$.

$$\alpha_{k,m} = \frac{C_k}{\left(IS_{k,m}^{RL} + \varepsilon\right)^2} \tag{16}$$

where $IS_{k,m}^{RL}$ is computed as follows.

$$IS_{k,m}^{RL} = \begin{cases} IS_{k,m}\, if\ \max(IS_{k,m}) / \min(IS_{k,m}) > 5 \\ 0 \qquad\qquad otherwise \end{cases} \tag{17}$$

With the above formulation, resolution of WENO scheme becomes higher as mapped technique. See Reference [14] for more details. This technique is also applied to WCNS and its efficiency is examined in this paper. This scheme is called WCNSRL.

2.4 Localization of Nonlinear-Weight Computation

Nonlinear-weight computation in the WCNS is computationally expensive because it includes transformation into characteristic variables. Therefore, the idea that the nonlinear-weight computation is localized only in non-smooth region seems better. Actually, this idea was introduced in original fifth-order WCNS by Deng and Zhang.[2] In this study, this idea is examined. For selecting non-smooth region, smooth indicator $IS_k^{density}$ for the density is used, where $IS_k^{density}$ is computed similar to eq. (11) for the density field. We use two limiters, absolute limiter and relative limiter as follows.

$$\frac{\max(IS_k^{density})}{\min(IS_k^{density})} > 5 \tag{18}$$

$$\max(IS_k^{density}) > 10^{-5} \times \rho_{ref} \tag{19}$$

Nonlinear weights are computed when both above two inequalities are fulfilled. For the smooth region where nonlinear weights are not used, following linear interpolation computed with ideal weights is used instead.

$$\begin{aligned} Q_{j+1/2}^{L} = \frac{1}{1024}(&-5Q_{j-3} + 42Q_{j-2} - 175Q_{j-1} \\ &+700Q_j + 525Q_{j+1} - 70Q_{j+2} + 7Q_{j+3}) \end{aligned} \tag{20}$$

This linear computation is computationally very cheap compared with nonlinear-weight computation. This reduces the computational cost very much. Note that relative limiter discussed before is also used, when this technique is employed. This scheme is called WCNSLNRL.

2.5 Compact Convex Combined Scheme

Yamashita and Maekawa introduced the compact convex combined scheme (CCCS).[15] This scheme uses following linear compact (implicit) interpolation in smooth region instead of eq. (20).

$$\begin{aligned} &\frac{1}{2}Q_{j-1/2}^{L} + Q_{j+1/2}^{L} + \frac{3}{14}Q_{j+3/2}^{L} \\ &\quad = \frac{1}{224}(-Q_{j-2} + 26Q_{j-1} \\ &\qquad\qquad + 210Q_j + 130Q_{j+1} + 7Q_{j+2}) \end{aligned} \tag{21}$$

For selecting non-smooth region, eqs. (18-19) are used. Note that relative limiter for non-linear weights discussed before are also used, when this technique is employed similar to WCNSLNRL. This scheme is called CCCSRL.

3 Evaluation with the Shock Entropy-Wave Interaction Problem

3.1 Problem Settings

The shock entropy-wave interaction problem is defined as follows.

$$(\rho, u, p) = \begin{cases} (3.857143, 2.629369, 10.333333) & x < -4 \\ (1 + 0.2\sin(5x)), 0, 1) & x \geq -4 \end{cases} \tag{22}$$

This problem is solved with WCNS with Roe's flux difference splitting method[8] and third-order total variation diminishing Runge-Kutta scheme[16], under CFL number 0.6 condition. Efficiency is defined as inverse of computational time under the same resolution, where computational time is normalized with

that of original WCNS. In this paper, reference solution is computed with ninth-order WCNS on 1601 grid points. This problem is computed on increasing grid points, which initiates 201 points, until the density $L2$ error compared with reference solution becomes lower than 0.05 for the solution of $1 < x < 2$, $t = 1.8$, at which high-frequency entropy wave is observed. When $L2$ error becomes lower than 0.05 for the first time, we define the same resolution for high-frequency waves. Inverse of the normalized computational time of this problem under the same resolution is defined as the efficiency ϕ_{1D} in a one-dimensional problem. Then, efficiency in a three-dimensional problem is simply estimated. From the test on 201 grid points, we can obtain ratio R_c of computational cost of schemes under the same grid points. From the tests on the same error, we can obtain ratio R_g of grid spacing of schemes under the same resolution. In a three-dimensional problem, ratio R_{NG3D} of grid points is inversely proportional to $(R_g)^3$ and ratio R_{NT3D} of total time steps is inversely proportional to R_g because of CFL number limitation. Ratio of computational cost for a three-dimensional problem on the same grid points is estimated based on above assumptions. Estimated efficiency ϕ_{3D} (inverse of estimated normalized computational time) of a three-dimensional problem is

$$\phi_{3D} = \frac{1}{R_c R_{NG3D} R_{NT3D}} = \frac{R_g^{3+1}}{R_c}. \qquad (23)$$

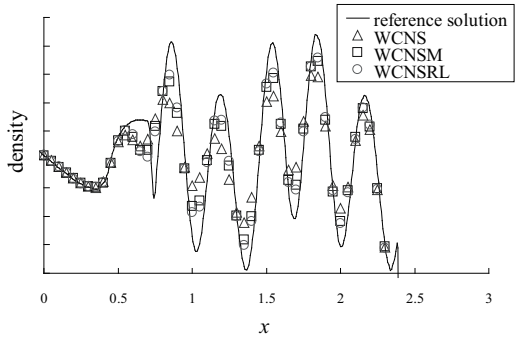

Fig.1: Comparisons of WCNS, WCNSM and WCNSRL with the shock entropy-wave interaction problem on 201 grid points.

3.2 Results

Figures 1 and 2 show the results with 201 grid points. Table 1 shows the computational time for 201 grid points, R_c, grid number for the same resolution, R_g, computational time for the same resolution, ϕ_{1D} and ϕ_{3D}.

Figure 1 shows that WCNSM and WCNSRL have higher resolution than original WCNS. Table 1 shows

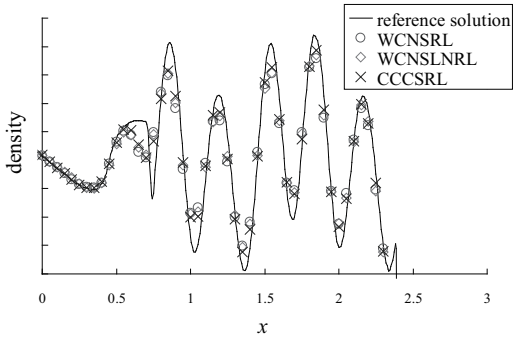

Fig.2: Comparisons of WCNSRL, WCNSLNRL and CCCSRL with the shock entropy-wave interaction problem on 201 grid points.

that the efficiencies ϕ_{3D} of WCNSM and WCNSRL are increased, while ϕ_{1D} of those are decreased. This shows that these techniques are worth employing for three-dimensional problems, but not for one-dimensional problems. In other words, saved cost by reducing grid points one-dimensionally is smaller than additional cost for these techniques, while saved cost by reducing grid points three-dimensionally is larger than additional cost for these techniques. Note that WCNSRL has slightly higher resolution than WCNSM.

Figure 2 shows that WCNSLNRL has slightly higher resolution than WCNSRL. This shows that localization of nonlinear-weight computation using eqs. (18,19) increases resolution as well as reduces computational cost shown in Table 1. As a result, computational efficiency (Table 1) is much increased using WCNSLNRL compared with WCNS.

Though CCCSRL has slightly higher resolution than WCNSLNRL as in Fig. 2, it does not appear in R_g (Table 1) compared with WCNSLNRL. As a result, CCCSRL has a slightly worse efficiency (Table 1) than WCNSLNRL because of additional computational cost.

A series of tests show that WCNSLNRL is the most efficient implementation in all schemes tested in this paper.

4 Application to Three-Dimensional Problems

In this section, WCNS and WCNSLNRL are applied to two practical three-dimensional problems. One is a supersonic jet impinging on an inclined flat plate and the other is a supersonic cavity flow.

Scheme	CPU time (sec) on 201 points	R_c	Grid number under same $L2$ error	R_g	CPU time (sec) under same $L2$ error	ϕ_{1D}	ϕ_{3D}
WCNS	0.135	1(ref.)	339	1(ref.)	0.379	1(ref.)	1(ref.)
WCNSM	0.187	1.39	299	1.13	0.41	0.92	1.19
WCNSRL	0.135	1.37	290	1.17	0.384	0.99	1.36
WCNSLNRL	0.076	0.56	269	1.26	0.122	3.11	4.49
CCCSRL	0.089	0.66	269	1.26	0.147	2.58	3.82

Table 1: Results for the shock entropy-wave interaction problem. (ref.) denotes the reference value for the row. Computations are conducted with Xeon 2.0GHz (1 core computation).

4.1 A Supersonic Jet Impinging on an Inclined Flat Plate

Flow and aeroacoustic fields of a supersonic circular jet impinging on an inclined flat plate are computed by WCNS and WCNSLNRL. Total number of grid points is 28 million. See Reference [17] for more details of computational conditions. Using WCNSLNRL, computational cost becomes three times lower than that of WCNS. Figures 3 and 4 show that the flow fields of WCNS and WCNSLNRL. These figures show that WCNSLNRL has higher resolution of aeroacoustic waves than original WCNS. Figure 5 presenting the probability of nonlinear-weight computation shows nonlinear-weight computation is only limited in turbulent shear-layer and shock region. This example shows that use of WCNSLNRL can reduce computational cost and improve resolution compared with WCNS.

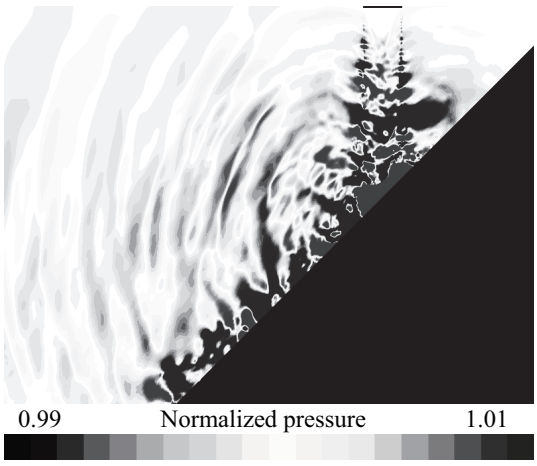

Fig.3: WCNS for a supersonic jet impinging on an inclined flat plate. An instantaneous pressure field.

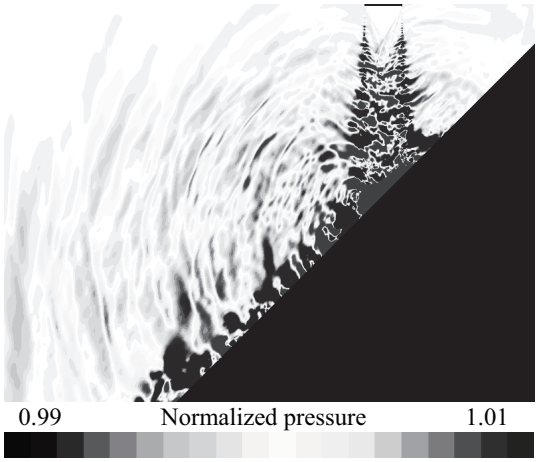

Fig.4: WCNSLNRL for a supersonic jet impinging on an inclined flat plate. An instantaneous pressure field.

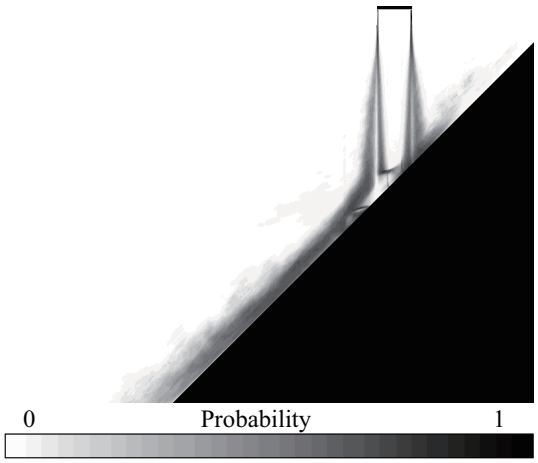

Fig.5: Probability of nonlinear-weight computation in WCNSLNRL for a supersonic jet impinging on an inclined flat plate.

4.2 A Supersonic Cavity Flow

Flow and aeroacoustic fields of a supersonic cavity flow are also computed by WCNS and WCNSLNRL. Total number of grid points is 7 million. See Reference [18] for more details of computational conditions. Using WCNSLNRL, computational cost becomes 1.5 times lower than WCNS. The reduction in computational cost is less than that of the previous computational case. This is because the nonlinear-weight-computation region is larger than that of the previous case. Figures 6 and 7 show that the flow fields of WCNS and WCNSLNRL. These figures show that WCNSLNRL has higher resolution of vortex structure than original WCNS. Figure 8 presenting the probability of nonlinear-weight computation shows nonlinear-weight computation is only limited in turbulent and shock region. This example also shows that use of WCNSLNRL can reduce computational cost and improve resolution compared with WCNS.

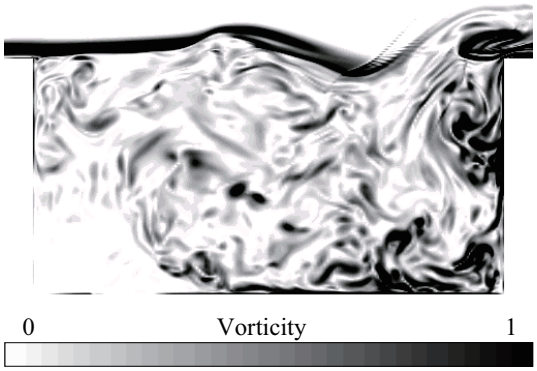

Fig.6: WCNS for a supersonic cavity flow. An instantaneous vorticity field.

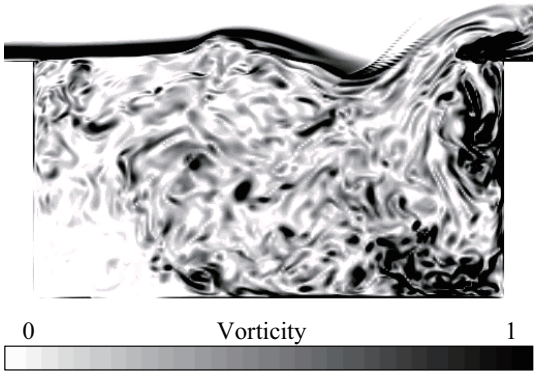

Fig.7: WCNSLNRL for a supersonic cavity flow. An instantaneous vorticity field.

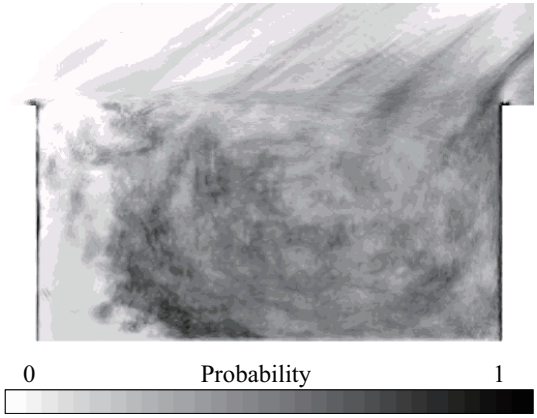

Fig.8: Probability of nonlinear-weight computation in WCNSLNRL for a supersonic cavity flow.

5 Conclusions

Efficient implementation of seventh-order WCNS is discussed with a one-dimensional shock entropy-wave interaction problem. Efficiency is defined as inverse of measured/estimated computational time under the same resolution. Use of mapping technique or relative limiter increases efficiency in a three-dimensional problem, but does not in a one-dimensional problem. Localization of nonlinear-weights computation and relative limiter for smooth indicator improve efficiency in one- and three-dimensional problems. Compact interpolation in smooth region does not increase efficiency in one- and three-dimensional problems. The present results show that use of both localization of nonlinear-weight computation and relative limiter for smooth indicator is the best choice for the supersonic turbulence computation.

REFERENCES

[1] Shu, C.-W., "High-order Finite Difference and Finite Volume WENO Schemes and Discontinuous Galerkin Methods for CFD," International Journal of Computational Fluid Dynamics, Vol.17, pp. 107-118, 2003.

[2] Deng, X. G. and Zhang, H., "Developing High-order Weighted Compact Nonlinear Schemes," Journal of Computational Physics, Vol.165, pp. 22-44, 2000.

[3] Shu, C.-W. and Osher, S., "Efficient Implementation of Essentially Non-oscillatory Shock Capturing Schemes," Journal of Computational Physics, Vol.77, pp. 439-471, 1988.

[4] Zhang, S., Jiang, S. and Shu, C-W., "Development of Nonlinear Weighted Compact Schemes with Increasingly Higher Order Accuracy," Journal of Computational Physics, Vol.227, pp. 7294-7321, 2008.

[5] Nonomura, T., Iizuka, N. and Fujii, K., "Freestream and Vortex Preservation Properties of High-order WENO and WCNS on Curvilinear Grids," Computers & Fluids, Vol. 39, pp. 197-214, 2010.

[6] Nonomura, T., Iizuka, N. and Fujii, K., "Increasing Order of Accuracy of Weighted Compact Nonlinear Scheme," AIAA paper 2007-893, 2007.

[7] Shu, C.-W. and Osher, S., "Efficient Implementation of Essentially Non-oscillatory Shock Capturing Schemes II," Journal of Computational Physics, Vol.78, pp. 32-78, 1989.

[8] Roe, P. L., "Approximate Riemann Solvers, Parameter Vectors, and Difference Scheme" Journal of Computational Physics, Vol.43, pp. 357-372, 1981.

[9] van Leer, B., "Flux-vector Splitting for the Euler Equations," Lecture Notes in Physics, vol 170, pp. 507-512, 1982.

[10] Liou, M. S. and Steffen, C. Jr, "A New Flux Splitting Scheme," Journal of Computational Physics, Vol.107, pp. 23-39, 1993.

[11] Liu, X., Deng, X. G. and Mao, M., "High-Order Behaviors of Weighted Compact Fifth-Order Nonlinear Schemes," AIAA Journal, Vol.45, pp. 2093-2097, 2007.

[12] Nonomura, T. and Fujii, K., "Effects of Difference Scheme Type in High-order Weighted Compact Nonlinear Schemes," Journal of Computational Physics, Vol.228, pp. 3533-3539, 2009.

[13] Henrick, A. K., Aslam, T. D. and Powers, J. M., "Mapped Weighted Essentially Non-oscillatory Schemes: Achieving Optimal Order Near Critical Points," Journal of Computational Physics, Vol.207, pp. 542-567, 2005.

[14] Taylor, E. M., Wua, M. and Martin, M. P., "Optimization of Nonlinear Error for Weighted Essentially Non-oscillatory Methods in Direct Numerical Simulations of Compressible Turbulence," Journal of Computational Physics, Vol.223(1), pp. 384-397, 2007.

[15] Yamashita, K. and Maekawa, H., "Direct Numerical Simulations of Hypersonic Boundary Layer Receptivity Using Compact Convex Combined Schemes," AIAA paper 2001-1798, 2001.

[16] Gottlieb, S. and Shu, C.-W., "Total Variation Diminishing Runge-Kutta Schemes," Mathematics of Computation, Vol.67, pp. 73-85, 1998.

[17] Nonomura, T., Goto, Y. and Fujii, K., "Acoustic Waves from a Supersonic Jet Impinging on an Inclined Flat Plate" AIAA paper 2010-476, 2010.

[18] Li, W., Nonomura, T., Oyama, A. and Fujii, K., "Numerical Study of Feedback-loop Mechanism of Supersonic Open Cavity Flows" AIAA paper, 2010, to be presented.